THE AMERICAN SOCIETY OF MECHANICAL ENGINEERS
345 E. 47th St., New York, N.Y. 10017

95-GT-146

RECENT ADVANCES IN GAS TURBINE ENGINE DYNAMIC MODELS DEVELOPED THROUGH JDAPS*

G. D. Garrard, M. W. Davis, Jr., and A. A. Hale
Sverdrup Technology, Inc.
1099 Avenue C
Arnold AFB, TN 37389-9013

ABSTRACT

The Joint Dynamic Airbreathing Propulsion Simulation (JDAPS) partnership was formed for the purpose of developing, validating, and applying advanced analytical simulations to investigate gas turbine engine dynamic performance and operability. This paper provides an introduction and demonstrates the operation of three dynamic models and simulations developed by members of the JDAPS partnership. These dynamic models and simulations include a new combustor analysis program (VPICOMB), the integration of the dynamic combustor model into an existing dynamic stage-by-stage compressor model and simulation (DYNTECC), and a new full gas turbine engine dynamic model and simulation (ATEC). For each of the gas turbine engine analysis tools, the model equations are first introduced, then operation of the simulation is demonstrated through selected test cases. The simulation results obtained during the operational verification test cases were appropriate for the inputs given. Calibration of the models and simulations has only been accomplished in a limited manner to date and will be the topic of future papers.

NOMENCLATURE

A	Area
D_0	Fuel Droplet Mean Diameter
F_x	Distributed Blade Force
H_{B_x}	Distributed Bleed Enthalpy
P	Pressure
Q_x	Distributed Heat Release Rate
R	Gas Constant
S_x	Distributed Shaft Work
SW	Shaft Work
T	Temperature
V	Volume
e	Internal Energy
f_c	Fraction of Air Entering Combustor Used in Combustion Process
$\dot{m}$	Mass Flow Rate
t	Time
u	Velocity
w_{B_x}	Distributed Bleed Flow Rate
x	Axial Coordinate
β	Fuel Droplet Evaporation Coefficient
ϕ	Equivalence Ratio
η	Efficiency
ρ	Density
τ	Time Constant

Subscript

ex	Exit
PZ	Zone of Heat Release
T	Total
in	Combustor Inlet
c	Combustor
L	Lean
R	Rich
s	Static
ss	Steady State

* The research reported herein was performed by the Arnold Engineering Development Center (AEDC), Air Force Materiel Command. Work and analysis for this research were done by personnel of Sverdrup Technology, Inc., AEDC Group, technical services contractor of the AEDC propulsion test facilities. Further reproduction is authorized to satisfy the needs of the U. S. Government.

Presented at the International Gas Turbine and Aeroengine Congress and Exposition
Houston, Texas - June 5-8, 1995

INTRODUCTION

The gas turbine engine has played a significant role in the advancement of the flight capabilities of modern day aircraft. The continuing demands for improved thrust and specific fuel consumption, however, have resulted in engine steady-state designs which are at or near the aerodynamic, thermal, and structural limits of the system components. In order for a gas turbine engine to operate at the performance, operability, and durability level for which it was designed, stable operation of the various engine components must be ensured (Khalid, 1992). Transient and dynamic instabilities which could push the engine components beyond their operating boundaries could result in loss of thrust, loss of engine control, or possible engine damage due to high heat loads and high cyclic stresses (Montgomery, 1971). The influence of operating instabilities must be quantified not only from the individual component considerations, but also from the point of view of any interaction between the various components.

One method that is available to the engineer to study dynamic engine behavior is to analytically evaluate the engine and component stability characteristics through mathematical models. The resulting models can then be tailored to a specific propulsion system through a validated numerical simulation. The Joint Dynamic Airbreathing Propulsion Simulations (JDAPS) partnership (Davis, et. al., 1995) was formed to provide the modeling capability to the various organizations working in the gas turbine engine industry. JDAPS is a partnership of government, university, and industry that was formed to develop and apply dynamic turbine engine and component numerical simulations to aid in the understanding of turbine engine dynamic behavior.

The JDAPS partnership has been in existence since 1991. Not only are state-of-the-art dynamic turbine engine models and simulations being developed, they are being applied to current turbine engine problems and analysis. A major benefit of JDAPS is its synergistic approach which combines each organization's financial and technical resources. This makes each organization's return on investment very high. Where technical talent is missing, another organization can be called upon to help fill the shortfall. By pooling resources and working together, JDAPS provides more resources than any one organization could afford.

The purpose of this paper is to describe three recent advances in modeling gas turbine engine dynamic behavior resulting from the JDAPS partnership. A dynamic turbine engine combustor model and simulation, VPICOMB, which was developed at Virginia Polytechnic Institute and State University, will be discussed. The integration of the VPICOMB combustion model equations with the DYNamic Turbine Engine Compressor Code (DYNTECC) conducted at the Arnold Engineering Development Center (AEDC) will then be discussed (Hale and Davis, 1992). Finally, a full gas turbine engine model and simulation, the Aerodynamic Turbine Engine Code (ATEC), also developed at AEDC, will be described. ATEC currently provides the capability to simulate a turbojet engine with the compressor system operating post-stall, and a turbofan engine operating up to the point of compressor stall.

GENERAL MODELING TECHNIQUE

The three models discussed herein each solve the one-dimensional Euler equations with turbomachinery source terms within a given domain of interest. In each model, the overall system under consideration is separated into individual control volumes, as is represented by the compressor system in Fig. 1. The governing equations are derived by the application of mass, momentum, and energy conservation to the elemental control volume and may be presented in the following form:

$$\frac{\partial}{\partial t}(QA) + \frac{\partial}{\partial x}(FA) = S$$

where:

$$Q = \begin{bmatrix} \rho \\ \rho u \\ e + \frac{1}{2}u^2 \end{bmatrix}; F = \begin{bmatrix} \rho u \\ \rho\left(u^2 + P\right) \\ \rho u\left(e + \frac{P}{\rho} + \frac{1}{2}u^2\right) \end{bmatrix}; S = \begin{bmatrix} -w_{B_x} \\ F_x \\ Q_x + S_x - H_{B_x} \end{bmatrix}$$

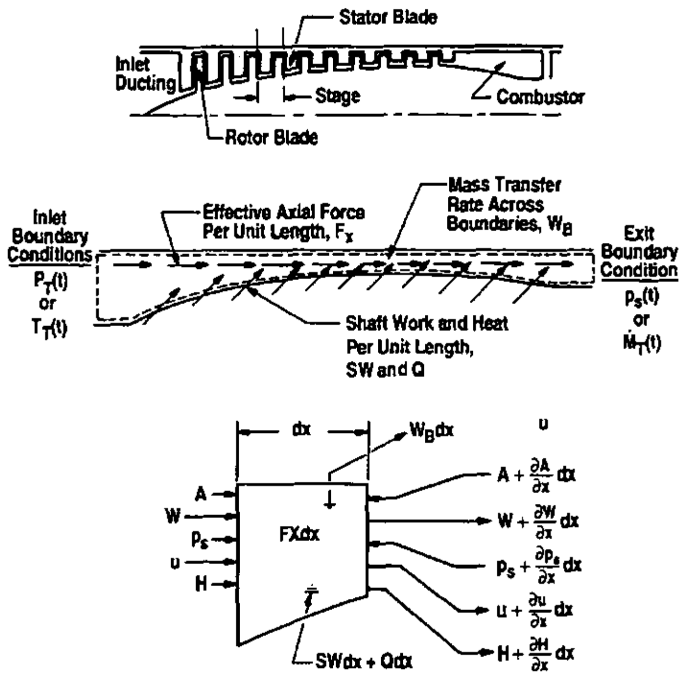

FIG. 1. SYSTEM DISCRETIZATION.

Additionally, a perfect gas is assumed and the equation of state $P = \rho RT$ is used. The assumption of constant c_p and γ in the property calculations, although computationally efficient, does result in predicted temperature levels in the combustor that are too high during rich combustion. This effect will be shown in the following sections.

The distributed turbomachinery source terms $\left(-w_{B_x}, F_x, Q_x + S_x - H_{B_x}\right)$ are supplied to the overall model by the user. Models for the source terms will be discussed in each of the respective sections.

The time-dependent flow field within the system of interest is obtained by solving the time-dependent system of equations using one of two numerical approaches. The VPICOMB model uses an explicit Roe's flux-differencing scheme adapted to the Euler's equations with source terms (Lindau and O'Brien, 1993) to evaluate the face fluxes, and then uses a second-order four-step Runge-Kutta algorithm to solve for the time-dependent equations. DYNTECC and ATEC use a flux-difference splitting scheme based upon characteristic theory (Varner, et. al., 1984) to solve for the face fluxes. A first-order Euler method is used to solve for the time-dependent equations.

SPECIFIC MODEL DESCRIPTION

VPICOMB:

The VPICOMB model and simulation provides a one-dimensional tool running on the personal computer for analyzing dynamic gas turbine engine combustor operation. With VPICOMB, the user can analyze the influence of varying inlet conditions, fuel pulses, exit flow restrictions, and many other possible dynamic events. The user provides the simulation with appropriate initial and boundary conditions, plus any time-dependent variations in the boundary conditions, and then exercises the program to determine the time-dependent flow field.

The solution process begins with the discretization of the combustor domain into individual control volumes as shown in Fig. 2. For the inlet boundary conditions, the user specifies inlet total pressure, total temperature, and flow rate. The friction factor along the wall of the combustor can also be specified by the user. No pressure loss due to combustion is assumed. The exit boundary condition assumes a constant value for the mass flow parameter:

$$\frac{W_{ex}\sqrt{T_{ex}}}{P_{ex}A_{ex}} = \text{Constant}$$

The value of the mass flow function is obtained during the initial conditions calculations.

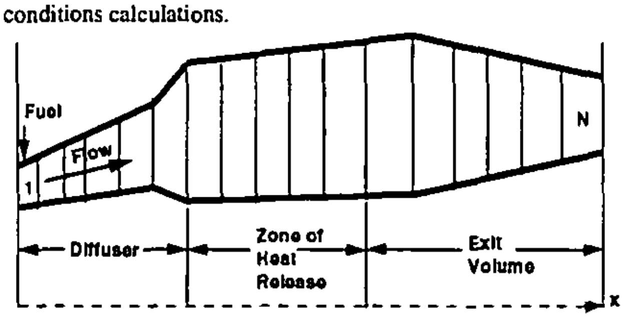

FIG. 2. COMBUSTOR DISCRETIZATION.

It is assumed that the fuel mass flow addition occurs in the first control volume. The heat release due to combustion occurs in the control volumes specified by the user as the zone of heat release. The heat release is equally distributed across the zone of heat release control volumes. The amount of energy released in the zone of heat release control volumes is a function of fuel flow rate, the combustion efficiency, the lower heating value of the fuel, and the combustor flammability limits.

The combustor flammability limits are determined by using steady-state engineering correlations developed by Herbert, 1957. For stable combustion to occur, the primary zone equivalence ratio (ϕ_{PZ}) must fall within a rich and lean limit:

$$\phi_L \le \phi_{PZ} \le \phi_R$$

Based on experimental data, Herbert defined a Combined Air Loading Factor to calibrate the light off and blow off data. A polynomial curve fit of Herbert's flammability data for a generic can-type combustor is used in the VPICOMB model. Combustion efficiency is determined by using steady-state engineering correlations developed by Lefebvre, 1985. Lefebvre assumed that the overall combustion efficiency is limited by the efficiency of fuel evaporation and the reaction efficiency. Further modification to the Lefebvre work following Derr and Mellor, 1990.

Because of the dynamic operation of the combustor, it is possible for heat release to occur for a short period of time, even though the combustor equivalence ratio may lie outside the steady-state flammability limits. Likewise, the heat release process may not resume immediately after the combustor equivalence ratio re-enters the flammability bounds. To account for these effects, a first-order lag on the heat release rate as proposed by Davis, 1986, is incorporated in the model:

$$\tau\frac{d\dot{Q}}{dt} + \dot{Q} = \dot{Q}_{ss}(t)$$

To demonstrate the operation of the model and simulation, a generic combustor was used. The geometry of the combustor is similar to that shown in Fig. 2. Inlet flow conditions were set such that stable operation of the combustor was obtained. Dynamic operation of the combustor was obtained by varying fuel flow rate while holding all other inlet boundary conditions constant. No friction losses were specified during this test run. The results of the simulation run are shown in Figs. 3 and 4. Fuel equivalence ratio in the primary zone of the combustor is shown in Fig. 3. The calculated upper and lower bounds on fuel equivalence ratio are also shown. The steady-state and time lagged heat release rates in the combustor as a function of time are shown in Fig. 4. Comparing the two figures clearly indicates that as the combustor fuel equivalence ratio becomes larger than the upper equivalence ratio limit, the combustion process is quenched. When the equivalence ratio re-enters the flammability region, the combustion process is reinitiated.

DYNTECC

DYNTECC is a one-dimensional, stage-by-stage compression system mathematical model and simulation capable of running on a personal computer or workstation (Hale and Davis, 1992). DYNTECC has proven itself to be of benefit by providing a tool to ana-

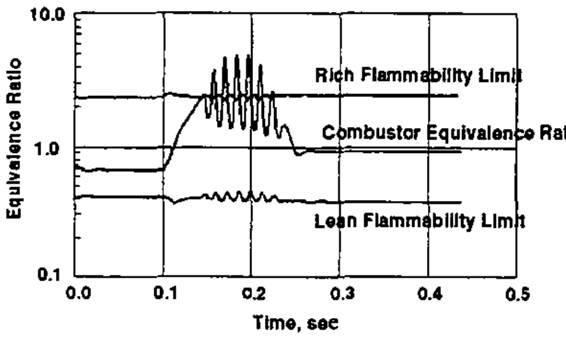

FIG. 3. EQUIVALENCE RATIO IN TEST COMBUSTOR.

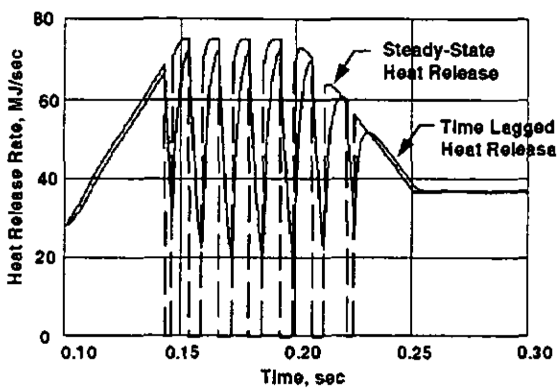

FIG. 4. HEAT RELEASE RATE FOR COMBUSTOR TEST CASE.

lyze dynamic compressor stability problems (Owen and Davis, 1994). Modified parallel compressor theory (Shahrokhi and Davis, 1995) has been applied to permit the simulation of dynamic inlet distortion. Source terms for blade forces and shaft work are obtained from user-provided steady-state compressor stage characteristics as shown in Fig. 5. Both pressure and temperature characteristics are required. During prestall operation, the steady-state compressor characteristics are used as given. During post-stall operation, the change in compressor operating conditions is lagged using the same first-order equation used in lagging the VPICOMB combustion heat release rate.

The most recent version of DYNTECC has been upgraded to include the VPI-developed combustor model discussed previously. This new feature will permit the user to study dynamic compressor/combustor interactions.

An example case using a single-spool, seven-stage axial and one-stage centrifugal compression system with no inlet distortion was chosen for demonstration. The geometry of the flow domain is shown in Fig. 6. The geometry and performance of the compressor system was based on results from a compressor rig test of the Lycoming T55 Turboshaft engine. A more detailed discussion of the rig test is given in Owen and Davis, 1994. A generic combustor was attached at the exit of the compressor system for this study. The system was operating initially with a combustor equivalence ratio of approximately 0.7. The test case demonstrates a 0.5-sec simulation with an arbitrary fuel flow increase of 25 percent occurring as is shown in Fig. 7. Inlet conditions to the compressor were set to sea-level-static conditions.

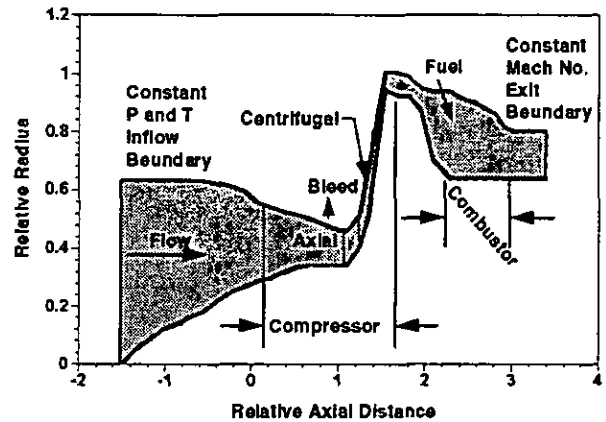

FIG. 6. COMPRESSOR/COMBUSTOR TEST CASE GEOMETRY.

Results of the test case are shown in Figs. 8 to 11. Relative total pressure through the system as a function of time, referenced to the compressor exit steady-state pressure, is shown in Fig. 8. Initially, the total pressure through the system from inlet to exit remains

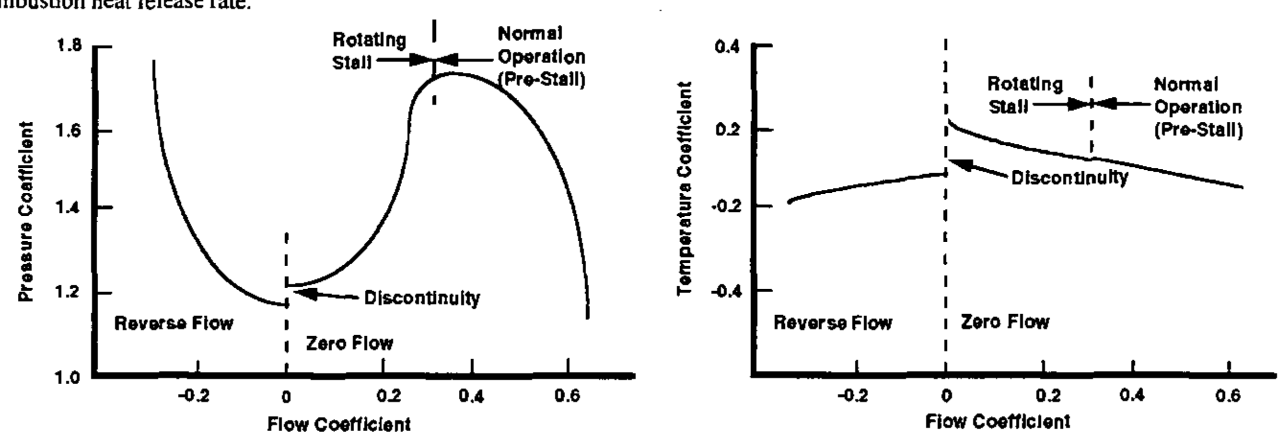

A. PRESSURE CHARACTERISTICS B. TEMPERATURE CHARACTERISTICS

FIG. 5. TYPICAL COMPRESSOR PRESSURE AND TEMPERATURE STAGE CHARACTERISTICS.

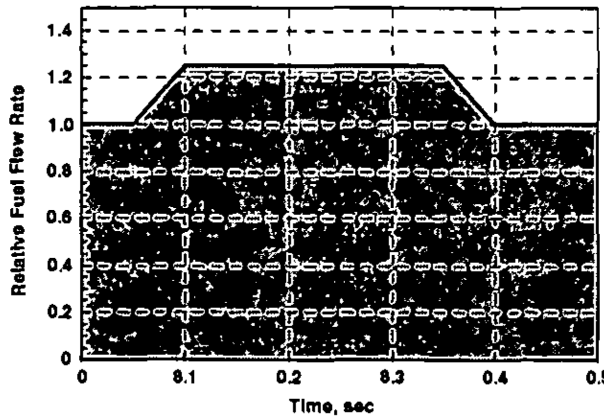

FIG. 7. FUEL FLOW VARIATION DURING COMPRESSOR/ COMBUSTOR TEST CASE.

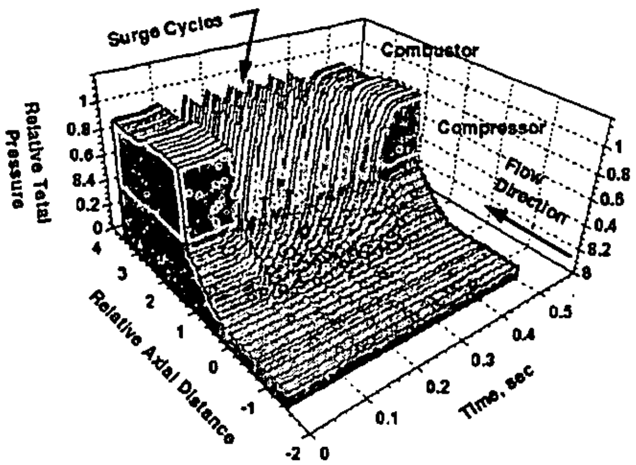

FIG. 8. TOTAL PRESSURE DURING DYNAMIC COMPRESSOR/COMBUSTOR EVENT.

steady, and the increase through the compressor system is broken into two sections. The axial compressor system provides a small percentage increase per stage. The centrifugal compressor, however, provides the bulk of the overall pressure rise in one model control volume. Total pressure downstream of the compressor increases with the start of the fuel flow rate ramp due to the reduced mass flow exiting the system. The reduced exit mass flow rate is the result of specifying a constant Mach number exit boundary condition. The increased fuel flow rate causes an increased flow temperature, which in turn causes the mass flow exiting the system to decrease in order to maintain the constant Mach number. The reduced flow and resulting pressure rise finally cause the compressor system to enter into surge. Steady-state operation is not reestablished until the fuel flow rate is reduced to the original value.

Relative total temperature through the system as a function of time, defined as the total temperature at a given location divided by the steady-state total temperature just downstream of the combustor, as shown in Fig. 9. As the flow passes through the system, total temperature increases through the compressor system due to the heat of compression. The bulk of the temperature rise occurs, however, in the combustor. As fuel flow is increased, the temperature likewise increases up to the point of combustor blowout. The variation of combustor exit temperature and time lagged heat release in the combustor primary zone as a function of time is shown in Fig. 10. As expected, there is a large increase in combustor exit temperature before blowout. This increase can be partially attributed to the reduced air flow rate and, hence, higher fuel equivalence ratio in the combustor. The doubling of the combustor exit temperature was not expected, however, indicating that improvements are needed in how DYNTECC determines the temperature of the flow. As noted

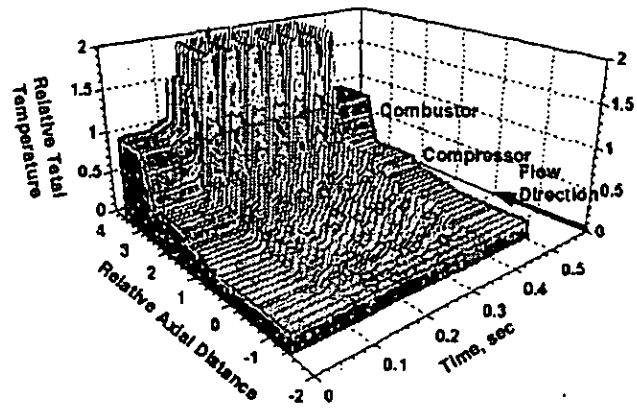

FIG. 9. TOTAL TEMPERATURE DURING DYNAMIC COMPRESSOR/COMBUSTOR EVENT.

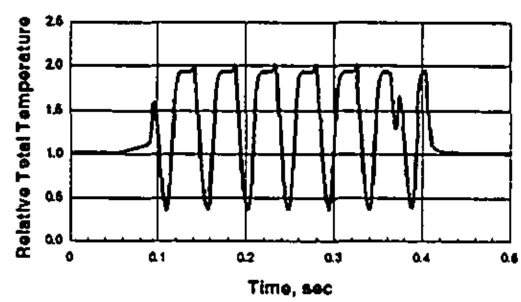

A. COMBUSTER EXIT TOTAL TEMPERATURE

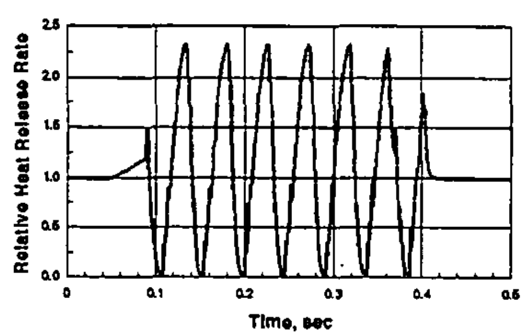

B. COMBUSTOR HEAT RELEASE RATE

FIG. 10. RELATIVE TOTAL TEMPERATURE AND RELATIVE HEAT RELEASE RATE IN COMBUSTOR DURING DYNAMIC COMPRESSOR/COMBUSTOR EVENT.

in the previous section, DYNTECC assumes constant c_p and γ in the flow calculations and as such cannot correctly handle the high-temperature regime. Improvements to the routine are under development.

Relative mass flow rate through the system as a function of time, referenced to steady-state inlet flow rate, is shown in Fig. 11. The initial mass flow rate through the system maintains a constant value through the system until the bleed flow is extracted in the compressor. Fuel addition occurs at the inlet to the combustor. During surge cycles, the mass flow rate in the system reverses through the compressor. However, downstream of the compressor, while the flow rate is greatly reduced, the mass flow rate does not actually reverse. The compressor system recovers from the surge cycle before the flow is forced to reverse in the combustor. To present this effect more clearly, time history plots of the relative mass flow rates just downstream of the compressor system and at the inlet to the combustor during a surge cycle are shown in Fig. 12.

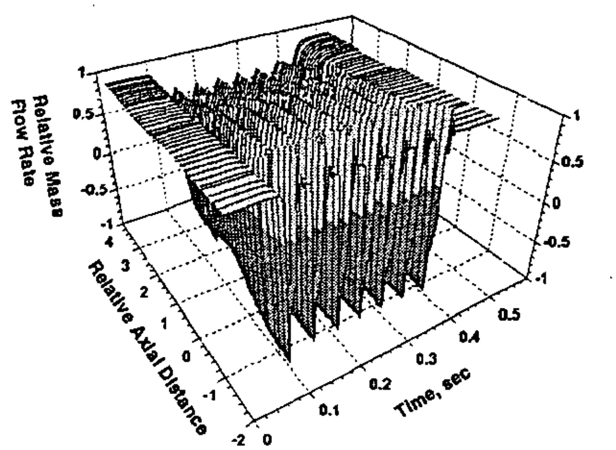

FIG. 11. MASS FLOW RATE VARIATION DURING DYNAMIC COMPRESSOR/COMBUSTOR EVENT.

ATEC

With the inclusion of the VPICOMB combustor model equations into the DYNTECC program, development of a gas turbine engine model and the required simulation was completed with the addition of a turbine model. Because of the modularity of the DYNTECC coding, integrating the turbine model into the existing code required specifying the performance characteristics in a fashion similar to the compressor performance (shaft work and blade forces). The turbine performance is provided to the simulation through turbine performance characteristics of the form shown in Fig. 13. Lines of constant corrected rotor speed are plotted, giving the turbine mass flow function as a function of turbine work done factor. The temperature ratio across the turbine is specified as a function of pressure ratio across the turbine. The temperature ratio versus pressure ratio characteristic is used rather than the more typical efficiency versus work done factor characteristic in order to provide robust simulation operation at low rotor speed. At low rotor

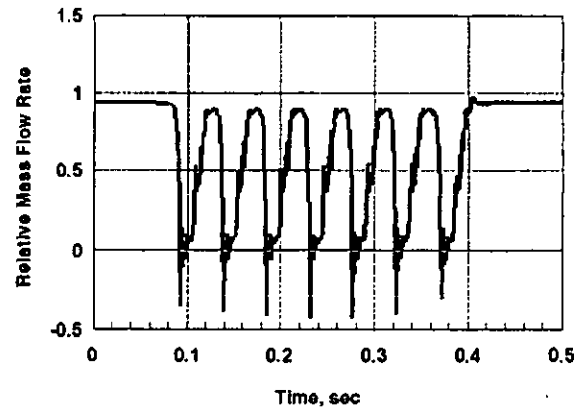

A. AT COMPRESSOR EXIT

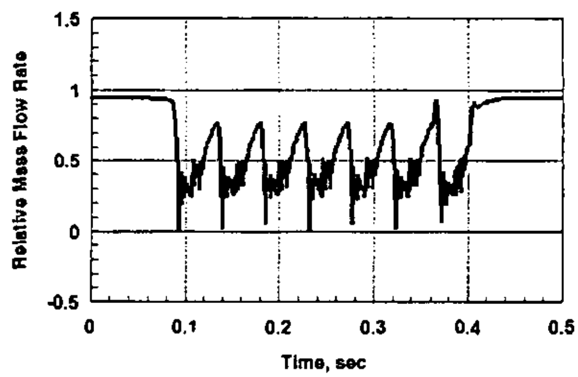

B. AT COMBUSTOR ENTRANCE.

FIG. 12. RELATIVE MASS FLOW RATE FOR DYNAMIC COMPRESSOR/COMBUSTOR EVENT.

speed, the efficiency approaches zero, while the temperature ratio and pressure ratio approach one. Choking of the turbine is obtained by limiting the mass flow rate through the turbine control volumes to the maximum value given by the steady-state turbine operating characteristics

ATEC is currently configured to support two gas generator turbines coupled to compressor systems through as many as two shafts and one power turbine. To determine the amount of work extracted across a given turbine during the initial conditions calculations, the gas generator turbine is assumed to exactly provide the power required by the compressor system. Work output from the power turbine is initially user-specified. Once the time integration starts, energy extraction is given by the pressure ratio across the turbine and the turbine inlet flow function.

Operational demonstration of the dynamic engine model was accomplished by using the T-55 Turboshaft engine. The calculation domain shown in Fig. 14 was derived from T-55 drawings. Because the turboshaft engine under consideration in this case has regions of the flow path that reverse direction and flow towards the front of the engine, the geometry does not appear as smooth as it might for an engine with a straight-through flow path. The volumes and linear distances have been matched to provide appropriate dynamic response. For this case, two turbines are modeled. The first turbine

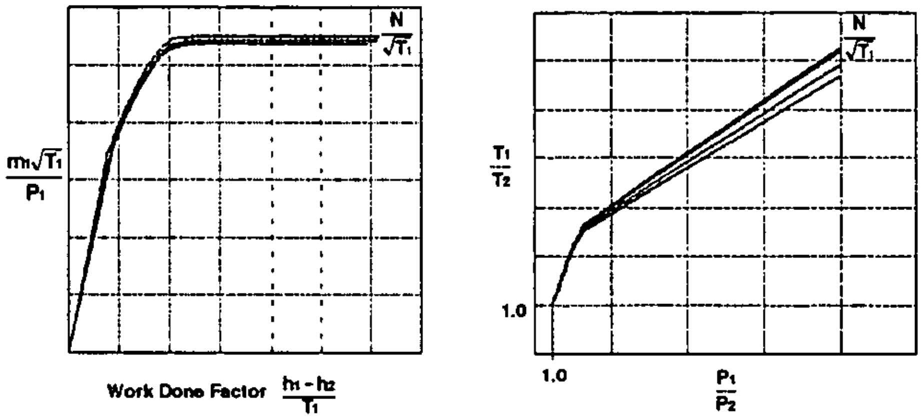

FIG. 13. TURBINE PERFORMANCE CHARACTERISTICS SPECIFICATION FOR ATEC.

is the gas generator turbine which is coupled to the compressor system, and the second turbine is the power turbine. Characteristics for each of the turbines are overall, not stage-by-stage, due to lack of interstage data. The shaft work and blade forces in each turbine were equally distributed across multiple control volumes, however, to keep the overall length of any given control volume on the same order as the rest of the grid. This helps maximize model dynamic fidelity and, with the explicit flow solver routine, numerical stability.

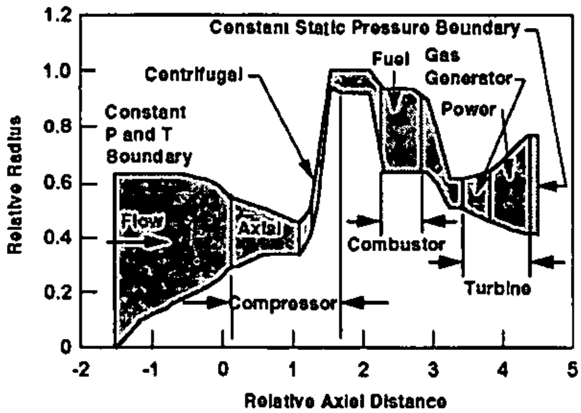

FIG. 14. GEOMETRY FOR ATEC TURBOSHAFT ENGINE TEST CASE.

Steady-state results of the engine system are compared to the engine manufacturer's steady-state engine model. The comparison results are shown in Table 1. Close agreement between the two models was obtained. It is judged that the majority of the differences can be attributed to the fact that the compressor characteristics for ATEC were based on compressor rig data, which was not the same as used in the steady-state model. Even with this difference, the maximum error was less than 7 percent

Table 1. Comparison of ATEC and Engine Model Result

Location	Total Pressure (P/Pref)			Total Temperature (T/Tref)		
	Mfg.	ATEC	%Delta	Mfg.	ATEC	%Delta
Inlet	0.29	0.29	0	0.26	0.26	0
Compressor Exit	2.38	2.38	0.73	0.51	0.51	0.72
Burner Exit	2.29	2.25	1.76	1.16	1.15	
Gas Generator Turbine Exit	0.81	0.87	-6.27	0.93	0.96	-3.63
Power Generator Turbine Exit	0.30	0.30	-0.75	0.75	0.79	-5.22

To demonstrate dynamic operation of ATEC, the same test case as was used to demonstrate the integration of the VPICOMB model equations into DYNTECC has been exercised. As in the previous case, the fuel flow to the combustor varied, as shown in Fig. 7.

Variation of the relative total pressure in the engine is shown in Fig. 15. During the initial steady-state operation, the total pressure increases through the compressor system. In the combustor, a small total pressure loss occurs. Work extraction in the turbines reduce the pressure to near atmospheric before the flow exits the engine. As with the DYNTECC test case, the fuel flow pulse forces the compressor into surge. Rather than being driven by a constant Mach number exit boundary condition, however, the pressure increase is tied to the turbine choking as explicitly defined by the turbine steady-state operating characteristics. Steady-state operation is not re-established until the fuel flow rate is decreased to the original flow rate. The frequency of the surge cycles is reduced due to the increased volume of the calculation domain.

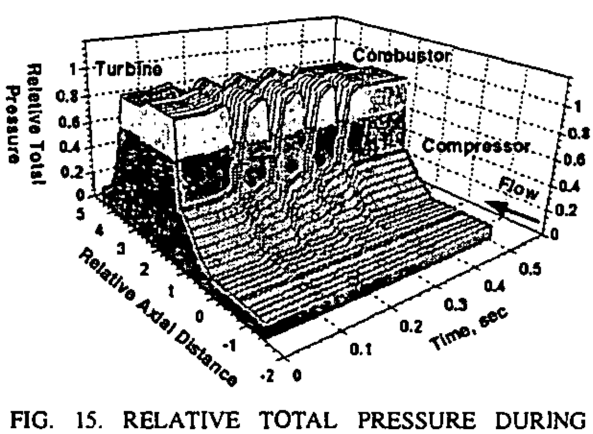

FIG. 15. RELATIVE TOTAL PRESSURE DURING DYNAMIC ENGINE EVENT.

Relative total temperature in the engine as a function of time is shown in Fig. 16. As the compressor enters the surge cycle, the reduction of air mass flow rate causes the combustor temperature to increase dramatically, until the equivalence ratio rises to the rich flammability limit. After the surge cycle is completed, the combustion process is re-established until the next cycle forces the equivalence ratio to rise above the flammability limit.

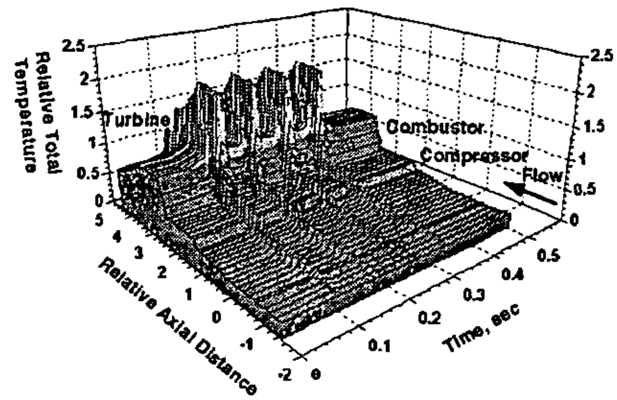

FIG. 16. RELATIVE TOTAL TEMPERATURE DURING DYNAMIC ENGINE EVENT.

Relative mass flow rate in the engine as a function of time is shown in Fig. 17. In addition to the bleed extraction occurring in the axial compressor and the fuel addition occurring in the combustor, turbine cooling bleed is injected into the flow in the last gas generator turbine control volume. As with the DYNTECC test case, during each of the surge cycles, the mass flow rate in the front section of the engine reverses and becomes negative. In the back section of the engine, the flow rate is greatly reduced, but it does not reverse.

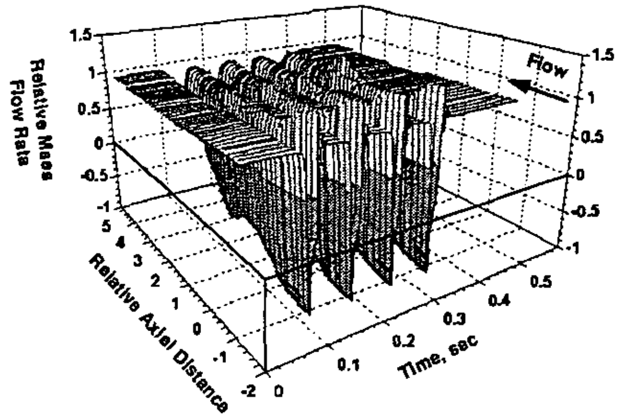

FIG. 17. RELATIVE MASS FLOW RATE DURING DYNAMIC ENGINE EVENT.

To demonstrate the capability of the model and simulation to simulate rotating stall in the compressor system, the above test case was repeated with a modification to the time lagging constant used with the compressor characteristics in the rotating stall regime. By increasing the time constant of each stage of the compressor system, the operational characteristics change. This results in the compressor system being unable to return to the normal operating mode. The effect is shown by comparing the compressor pressure ratio curves as a function of mass flow rate through the system for both cases. This comparision is shown in Fig. 18. With a relatively small time constant, the dynamics of the system allow the compressor to return to the normal prestall operating speed line before reentering the surge cycle, as is shown in Fig. 18a. As is shown in Figs. 15 - 17, once the perturbation in fuel flow rate is removed, the system returns to normal, steady-state operation. An increase in the compression system time constants forces the system into rotating stall, as is shown in Fig. 18b. Even when the fuel flow rate is reduced to the original level, the system is unable to recover to the original steady-state operating point. The relative pressure through the engine system is shown in Fig. 19.

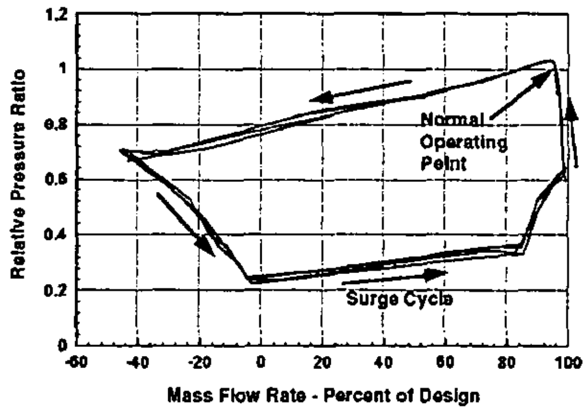

A. SURGE CYLE - SMALL LAGGING CONSTANT

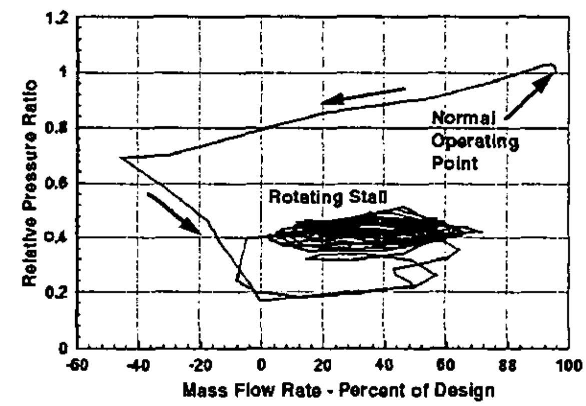

B. ROTATING STALL - LARGER LAGGING CONSTANT
FIG. 18. COMPRESSOR OPERATION MAPS FOR DIFFERENT SYSTEM RESPONSES.

SUMMARY

This paper has described three recent advances in the modeling of gas turbine engine dynamic behavior. These advances have come from members of the JDAPS partnership. The advances discussed herein are:

- A dynamic turbine engine combustor model and simulation (VPICOMB)

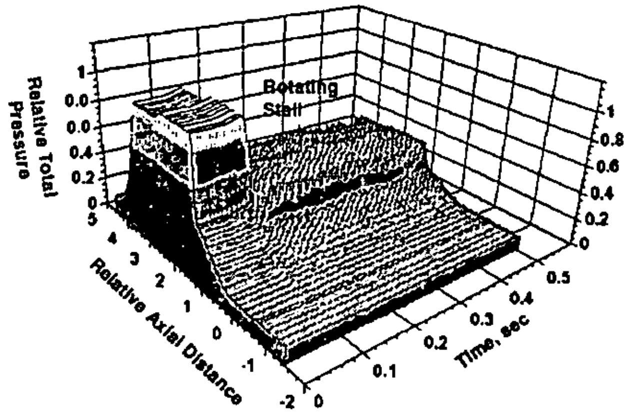

FIG. 19. RELATIVE TOTAL PRESSURE IN ENGINE DURING DYNAMIC ROTATING STALL EVENT.

- The integration of the combustor model into an existing dynamic compressor system model and simulation (DYNTECC)
- A dynamic full gas turbine engine model and simulation (ATEC)

These three dynamic simulations have been operationally verified for selected test cases. All of the models and simulations appear to exhibit qualitatively correct behavior for the cases considered. Calibration to test data must be accomplished, however, and is currently in progress.

Further improvements and development of new models and simulation will be occurring through the JDAPS partnership. Of equal importance to the model development, and the focus of all members of the JDAPS partnership, is model calibration. DYNTECC, with the many applications to which it has been applied, has received the greatest amount of calibration. Calibration is a never-ending process, however, and the results of the calibration efforts will be reported as they become available.

REFERENCES

Davis, M. W., "A Stage-by-Stage Post-Stall Compressor System Modeling Technique: Methodology, Validation, and Application," Ph.D. Dissertation, Virginia Polytechnic Institute and State University, August 1986.

Davis, M. W., Jr., Owen, A. K., O'Brien, W. F., and Cousins, W. T., "Joint Dynamic Airbreathing Propulsion Simulations Partnership JDAPS," ASME Paper to be presented at the 40th ASME International Gas Turbine and Aeroengine Congress and Exposition, Houston, TX, June 1995.

Derr, W. S. and Mellor, A. M., "Recent Developments," in *Design of Modern Turbine Combustors*, Edited by A. M. Mellor, Academic Press, Harcourt Brace Jovanovich, New York, 1990.

Hale, A. A. and Davis, M. W., "DYNamic Turbine Engine Compressor Code DYNTECC - Theory and Capabilities," AIAA-92-3190, AIAA/SAE/ASME/ASEE 28th Joint Propulsion Conference and Exhibit, Nashville, TN, July 6-8, 1992.

Herbert, M. V., "A Theoretical Analysis of Reaction Rate Controlled Systems - Part 1," Chapter 6 in *Combustion Research and Reviews*, 1957, Agardograph No. 15, Butterworths Scientific Publications, London, England, February 1957.

Khalid, S. J., "Role of Dynamic Simulation in Fighter Engine Design and Development," *AIAA Journal of Propulsion*, Jan.-Feb. 1992, pp. 219-226.

Lefebvre, A. H. "Fuel Effects on Gas Turbine Combustion - Ignition, Stability, and Combustion Efficiency," *Journal of Engineering for Gas Turbines and Power*, Vol. 107, January 1985, pp. 24-37.

Lindau, J. W. and O'Brien, W. F., "Solution Schemes for Stage by Stage Dynamic Compression System Modeling," AIAA 93-0154, 31st Aerospace Sciences Meeting and Exhibit, Reno, NV, January 11-14, 1993.

Montgomery, J. F., III, "The Need for Air Force Engine Stability Margin Testing for Inlet-Engine Interface Definition," AFAPL TR-71-84, December 1971.

Owen, A. K. and Davis, M. W., Jr., "Modeling the Dynamic Behavior of an Axial-Centrifugal Compression System," AIAA-94-2802, 30th AIAA/ASME/SAE/ASEE Joint Propulsion Conference, Indianapolis, IN, June 27-29, 1994.

Shahrokhi, K. A. and Davis, M. W., Jr., "Application of a Modified Dynamic Compression System Model to a Low-Aspect Ratio Fan: Effects of Inlet Distortion," AIAA 95-0301, 33rd AIAA Aerospace Sciences Meeting and Exhibit, Reno, NV, January 9-11, 1995.

Varner, M. O., Martindale, W. J., Phares, W. J., Kineile, K. R., and Adams, J. C., "Large Perturbation Flow Field Analysis and Simulation for Supersonic Inlets," NASA CR-174676, September 1984.

ACKNOWLEDGEMENTS

The work reported herein was jointly supported by the Arnold Engineering Development Center, AF/DOT, the Army Vehicle Propulsion Directorate, NASA, Lewis Research Center, and AlliedSignal who supported Virginia Polytechnic Institute and State University under the Joint Dynamic Airbreathing Propulsion Simulation (JDAPS) Partnership.